Topographic Templating of Islands and Holes in Highly Asymmetric Block Copolymer Films

Rachel A. Segalman,[†] Kathleen E. Schaefer,[‡] Glenn H. Fredrickson,[†] and Edward J. Kramer*[,‡,†]

Departments of Chemical Engineering and Materials, University of California, Santa Barbara, California 93106-5050

Sergei Magonov

Digital Instruments-Veeco Metrology Group, Santa Barbara, California 93117

Received November 26, 2002; Revised Manuscript Received February 14, 2003

ABSTRACT: Asymmetric diblock copolymers with a spherical domain structure form islands or holes on the free surface of a thin film when the initial spun-cast film thickness does not match that of an integral number of layers of spheres plus a brush. When this film is cast on a substrate topologically patterned with rectangular, flat bottomed wells as deep as a layer of spheres, the edges of these wells act as sinks for excess material. As a result, we observe the movement of material away from the raised areas (mesas) toward the adjacent wells so that if a mesa surface initially contains holes exposing the underlying layer of spheres or brush, these holes will coalesce and grow until the top layer of spheres forms a bicontinuous structure with the holes, and finally this structure will break up into discrete islands. If the islands exist on top of only a brush layer, their shrinkage is limited by the detachment kinetics of a chain from the island into the brush. If the islands are on top of another layer of spheres, the shrinkage of the islands is much faster than would be expected if it were controlled by the diffusion of chains through the underlying nanodomain structure.

Introduction

Thin films of block copolymers have been much explored for applications ranging from nanolithography[1−6] to the templating of inorganic structures such as nanowires and magnetic dots.[7−10] They hold unique promise in these fields because they microphase separate into a variety of nanoscale structures. The shapes of these nanodomains range from spheres to lamellae as the block fraction, f, increases from 0 to 0.5, and the sizes of these highly uniform nanodomains can be controlled by adjusting the total chain length, N.[11] The presence of a directional field (electric, magnetic, or surface energy) can orient lamellar or cylindrical nanodomains in a film.[12−17] The placement of nanodomains may be controlled by epitaxially templating the substrate on the size scale of the nanodomains[18] or by graphoepitaxy.[19] All of these methods, however, require a detailed understanding of effects of surfaces and interfaces on the thin film.

The dependence of the orientation of lamellar and cylindrical block copolymer nanodomains on the thickness has been well studied and is covered in a recent review.[20] A difference in block interfacial energies will attract one of the blocks to the substrate, inducing a layering effect on the remainder of the film.[21−26] Lamellar films possess a natural repeat spacing of the domain structure, L_0, and pay a free energy penalty due to chain stretching or compression when the film thickness is not commensurate with this spacing. This results in the generation of islands and holes (surface structures) at the polymer/air interface. Smooth films are observed after annealing above the glass transition only when the original, spun-cast film thickness matches a natural thickness, h.

When both surfaces attract the same block, h is equal to nL_0 where n is an integer. When the two interfaces attract different blocks, flat films only occur when the initial film thickness equals $(n + {}^1/_2)L_0$. Recently, surface patterning has been employed by several groups to control island structures. For sublamellar thickness films, physical patterning (creating thickness modulation of the overlying polymer film)[27] as well as chemical patterning[28] of the substrate with repeat spacings on the lamellar size scale have dramatic effects on lamellar structure and orientation. Heier et al. have succeeded in templating surface domain structures on smooth substrates that were chemically patterned by microcontact printing on a scale of 1−16 μm.[29]

Initially, islands and holes form randomly over the sample surface. While studies of the early stage development of block copolymer lamellae islands are rare, it appears that the formation of islands from an initially disordered film occurs by a process analogous to spinodal decomposition.[30,31] The kinetics of the later stage growth of these surface structures has been studied in much greater detail and has been analyzed as an Ostwald ripening process.[32−39] Typically, the average size of the islands increases through coalescence of smaller domains and the growth of larger domains at the expense of smaller ones. This coarsening is driven by the line tension of the edges of the 2-D islands so that over time there is a decrease in the total length of island edges. There are three possible mechanisms by which a small island can shrink: (a) the diffusion tunneling of individual chains through the lamellar structure away from the island, (b) the diffusion of an entire island on the surface until it encounters and

[†] Department of Chemical Engineering.
[‡] Department of Materials.
* To whom correspondence should be addressed: e-mail edkramer@mrl.ucsb.edu, tel (805) 893-4999.

10.1021/ma025879c CCC: $25.00
Published on Web 05/15/2003

coalesces with another island, or (c) the viscous flow of chains along a continuous path created by a defect in the lamellar structure within the islands.[40] Heier et al. templated the structure of islands of strongly segregated, lamellae forming block copolymer using an underlying periodic chemical structure on the substrate formed by microcontact printing. By watching the disappearance of isolated islands near an absorbing boundary, they were able to conclude that the primary mechanism of island shrinkage is the flow of chains through defect structures in the lamellae (mechanism c above).[41]

When a film of a sphere forming poly(styrene-*b*-2-vinylpyridine) (PS−PVP) diblock copolymer is deposited on a flat silicon oxide substrate, the difference in surface energy in the two blocks leads to layering of the spheres with layers parallel to the substrate, similar to that observed in lamellar block copolymers.[42] For a thin enough film (five layers or less), this layering in turn leads to a quantization in the film thickness in the ordered state. Islands and holes form when the film thickness does not closely match a natural thickness given approximately by

$$h = \alpha n + \beta \tag{1}$$

where α is the distance between layers of spheres and β is the thickness of a brush adsorbed on the substrate surface if such a brush forms. Slight changes in thickness result in surface relief structures, just as they do in a lamellar block copolymer system. The coarsening of these structures, however, must occur through fundamentally different mechanisms than the mechanism (c) observed in the lamellar block copolymer systems. The viscous flow of chains through defect structures is not possible in the spherical nanophase since there are no continuous block copolymer interfaces.

In this paper, we will demonstrate that, by using a topographically patterned substrate, we can create sinks for excess material. If we create a series of rectangular depressions (wells) on an otherwise flat silicon oxide substrate, excess material may be transferred to the well, leading to a decrease in the total island edge length. In this manner, it is possible to pattern the island or hole formation. We find that as the sink absorbs material from the surrounding mesas, holes on the mesa will coalesce to form a bicontinuous structure which will thin into individual islands which will finally dissolve to leave behind a flat structure. The rates of shrinkage of individual islands on top of the brush were far different than those of islands on top of another layer of spheres. When the film contains less than a single layer of spheres, chains must detach from the island and then diffuse across a dense brush to the sink. By contrast, when the film contains more than one layer of spheres, islands dissolve much more quickly. The speed of this island dissolution is much faster than would be expected for the diffusion of chains through the spherical nanodomains but may be indicative of the absorption of excess material into dislocations or grain boundaries in the underlying film.

Experimental Section

Silicon wafers were obtained from Cypress Semiconductor Corp. (Minneapolis, MN) and coated with a 30 nm thick layer of silicon oxide by electron beam evaporation. The substrates were then patterned by photolithography and chemical etching with hydrofluoric acid to produce a series of long (1 mm) mesas ranging in width from 1 to 15 μm separated by wells of equal width. A native oxide layer (2−3 nm) was allowed to regrow on all etched surfaces. This final structure consisted of a SiO_2 surface patterned with raised mesas 30 nm higher than the adjacent wells.

The PS−PVP block copolymer was synthesized by anionic polymerization as previously documented[42] and had a total degree of polymerization $N = 670$ and a PVP mole fraction of 0.129. In the bulk, this material self-assembles into PVP spheres of 9 nm in diameter arranged in a body-centered-cubic (bcc) array with a (110) plane spacing of 27 nm surrounded by a PS matrix. Thin films initially spun cast from dilute (~1%) toluene solution onto glass microscope slides are disordered and do not form spheres. Thickness was controlled by modifying the solution concentration and spin speed. The glass slides were slowly immersed in deionized water immediately after spin coating. The intrinsic layer of surfactant on the glass surface released the disordered block copolymer thin films to the air/water interface where they were retrieved on top of the patterned silicon substrates.

All samples were normally annealed at 180 °C in a vacuum $<10^{-6}$ Torr to order the block copolymer nanodomains and allow the formation of islands and holes. After annealing, a 20 nm PVP−PS brush at the silicon oxide surface overlaid by layers of PVP spheres encased in a PS matrix was observed.[43] Changes in island and hole shape and size were observed in real time by annealing films on an Instec HCS600V heat stage on an optical microscope. The heat stage was operated at 180 °C under a constant purge of ultrahigh-purity N_2 gas which had been further purified in a zeolite molecular sieve column produced by Mettler. More detailed images were obtained by following a similar procedure on the high-temperature stage of a Digital Instruments MultiMode AFM. In this case, the films were annealed at 180 °C in a helium environment. In both cases, images were taken periodically during a 5 day annealing cycle.

Results and Discussion

Lateral confinement within a substrate topography can align the spherical nanodomains of an asymmetric diblock copolymer film. This substrate topography can also template the larger surface structures (islands or holes) that are created when the initial film thickness does not match that of an integral number of sphere layers plus brush. There is a further interplay between the orientation and order of the island or hole structures and the ordering of the arrays of spherical nanodomains.

Templating of Islands and Holes. When the initial spun-cast film thickness, *th*, is 47 nm, a PS−PVP brush with $\beta = 20$ nm and a single layer of spheres with $\alpha = 27$ nm form after annealing at 180 °C for 72 h. As shown in Figure 1, the spheres in this layer continue to conform to the underlying substrate pattern so an unetched film appears to be smooth, and the only surface topographies visible are the 30 nm steps templated by the substrate.

When the film thickness deviates slightly from 47 nm, surface structures form either holes revealing the underlying brush when $th < 47$ nm or islands of an extra layer of spheres when $th > 47$ nm. On a flat substrate both islands and holes are driven to coarsen by the line tension of their edges. The block copolymer at the edge of a hole has a negative chemical potential, μ_{hole}, inversely proportional to the local radius of the hole, R_{hole}:

$$\mu_{hole} = -\frac{\gamma_{edge} N}{R_{hole} \rho} \tag{2}$$

where γ_{edge} is the surface tension of the edge of each hole and ρ is the mer number density. The block

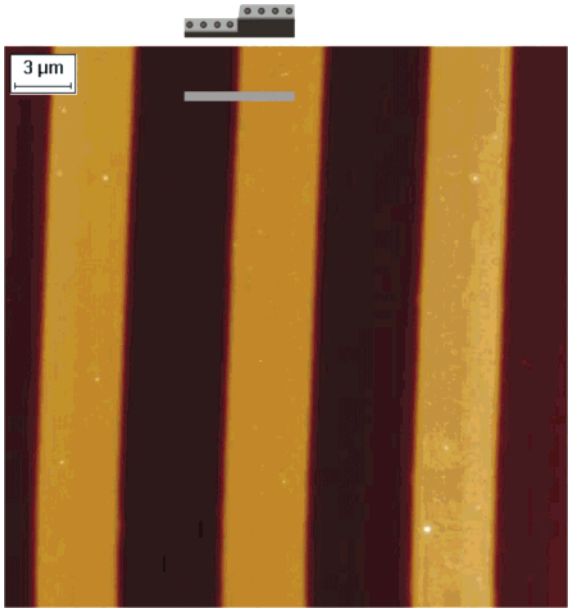

Figure 1. When the spun-cast film is 47 nm thick, after annealing all surfaces are covered with a brush and one layer of spheres. The SFM image shows the relatively straight edges of the mesa and well on a 75 nm height scale (dark to bright). At the location of the gray line on the image, the film will have a cross section similar to the schematic.

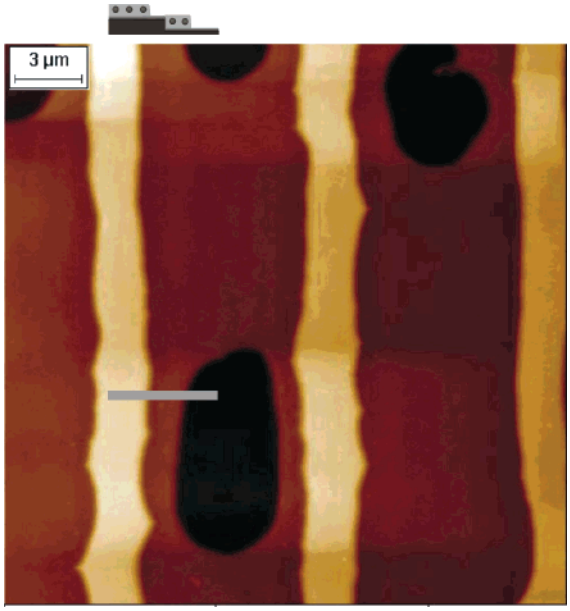

Figure 2. Wells are preferentially filled when the initial film thickness is less than that necessary to form a brush and an entire layer of spheres. After annealing for 72 h at 180 °C, the islands have dewet the edges of the mesa to reveal a brush and the spheres almost completely fill the wells. The SFM image shows the topography with a 75 nm height scale (dark to bright). At the location indicated by the gray line on the SFM image, the film has a cross section as schematically indicated.

copolymer at the edge of an island has a positive chemical potential opposite in sign to eq 2 but with the same dependences on γ_{edge}, ρ, N, and R_{island}.

The substrate mesas, however, are exactly one sphere high and can be viewed as artificial islands. The edges of these long, narrow islands are straight ($R \rightarrow \infty$) so the block copolymer chemical potential at the edge of the mesa is

$$\mu_{mesa-edge} = 0 \tag{3}$$

Because of the differences in chemical potential, the mesa edge acts as a sink for block copolymer from the islands and a source of block copolymer for the holes.

For all films with $th < \alpha + \beta$ (47 nm) thick, the holes in the sphere layers in the wells are sinks for the spheres from the mesa and eventually fill at the expense of the mesa. This transport of block copolymer effectively widens the well and decreases the total edge line length. As a result, after 72 h of annealing, a film with initial thickness, $th = 42$ nm, has shrunk away from edges of the mesa to reveal the underlying brush, as shown in Figure 2. The wells have filled with material at the expense of the mesa; though after 72 h, this process is not yet complete, and a few large holes still exist in the well. Since the wells are not exactly 27 nm deeper than the nearby mesas and are filled with a 27 nm thick layer of spheres, a slight height differential is observed at the mesa/well interface. In the situation depicted in Figure 2, there is enough material left on the mesa to form a long narrow ribbon on the center of the mesa. The arrangement of the block copolymer spherical nanodomains is templated via graphoepitaxy in the well by the hard silicon oxide step and on the mesa by the vacuum edges of the long narrow strip of material.[19] If more material is needed to fill the well, the residual island stripe on the mesa breaks up eventually into discrete islands. This breakup is reminiscent of a Raleigh instability wherein a fluid cylinder whose length is much greater than its circumference breaks into droplets.[44] This instability is the triggered by small perturbations of long wavelengths. As expected, the islands on the mesa are only seen to be susceptible to breakup when they are sufficiently narrow. This results in a straight line of regularly sized islands along the center of the mesa, reminiscent of the droplets that remain after the breakup of a rim after polymer thin film dewetting.[45,46]

As shown in Figure 3, if the initial film thickness is slightly greater than 47 nm, the wells still act as sinks for the excess material on the mesa. In this case, if the island material exists at the well edges, it can extend the width of the mesa without creating any extra line length. The edges of the well now contain two layers of spheres while the mesa and the center of the well contain only one layer of spheres plus a few sporadic islands. Again, the height of the mesa does not exactly match the depth of a single layer of spheres so there is a small height differential at the mesa/well interface visible in the SFM micrograph in Figure 3.

It follows, therefore, that if th exactly equals $1.5\alpha + \beta$, the wells can be filled completely with two layers of spheres while the mesa will contain only one layer of spheres. In this case, the polymer will nearly mask the substrate templating and appear to be flat, as shown in Figure 4. Again, there is a slight mismatch in the mesa height and the filled well, visible as a step of <1 nm in the SFM image. By etching this film with secondary ion mass spectroscopy (as previously documented[19]), we can reveal the nanodomain order of this apparently flat film and then determine the in-plane order with SFM (not shown). Both the single layer of spheres on the mesa and the two layers of spheres in the well show characteristics of graphoepitaxy. A single grain with a hexagonal structure persists for at least 1.5 μm from either templating edge.[19]

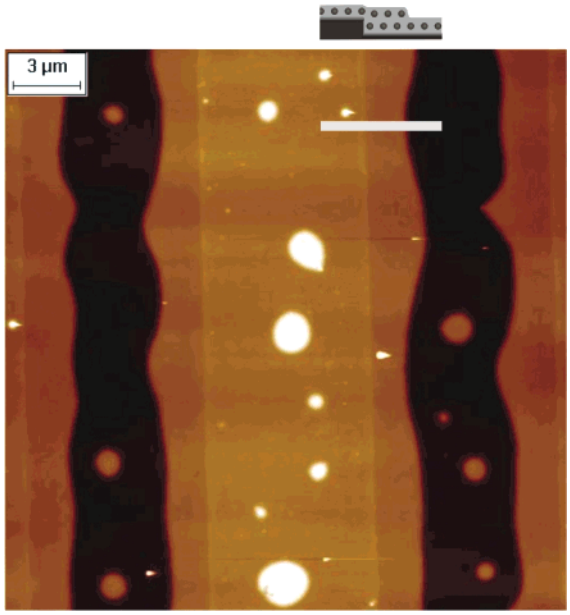

Figure 3. If the film thickness is slightly over 47 nm, the excess material is preferentially moved toward the edges of the well where no extra island edge length is necessary, as shown in the schematic. The SFM image demonstrates that after 72 h of annealing some small islands still remain on the mesa.

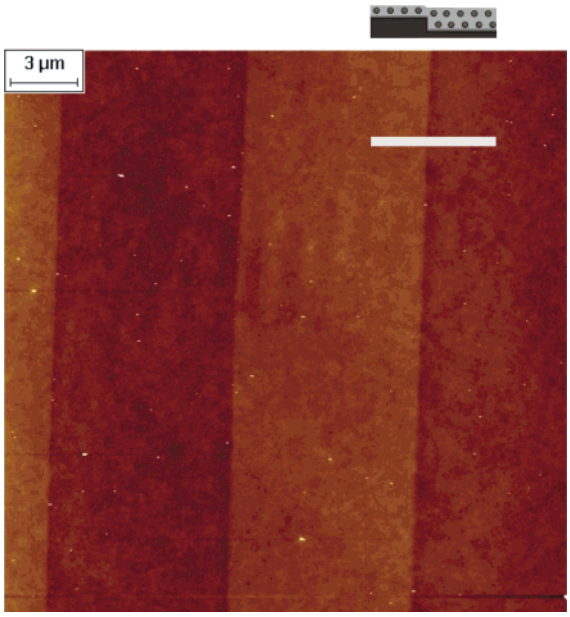

Figure 4. If the film thickness is exactly $\beta + 1.5\alpha$, the well can be completely filled with the extra half layer of material so that the total height scale is of this image is only 10 nm. The gray line indicates the location of the schematic cross section.

In films on flat substrates, there is a relatively large initial film thickness range in which the film will consist of a single layer of spheres on all surfaces. This is because each surface structure (island or hole) will require some line length and therefore some additional surface energy. On the other hand, the addition of extra spheres to the edge of the mesa or the subtraction of spheres from this edge of our topographically structured substrates creates no additional line length or surface energy. As a result, it is very difficult to create a film as shown in Figure 1 where exactly one layer of spheres covers all surfaces. Instead, it is relatively easy for the material to shrink slightly from the edges of the mesa or for material to slightly spill over the edges to create a partial extra layer of spheres on the well. Our previous studies on the melting of 2-D arrays of block copolymer spherical nanodomains were performed on films that were just slightly underfilled so that the sphere layer shrank slightly back from the edges of the mesa.[43,47,48]

Graphoepitaxy has been proposed as a mechanism for nanopatterning substrates for applications in memory storage devices. The fact that the polymer film responds to substrate topography on two distinct length scales, that of the spherical nanodomains and the much larger size scale of island and holes, indicates that additional care must be taken in coordinating substrate design with film thickness. For instance, a substrate patterned with long, narrow mesas and wide wells and slightly underfilled with block copolymer would result in wells filled with single crystalline block copolymer arrays separated by empty mesas. It would be much more difficult, however, to cover all surfaces of a patterned substrate with exactly one layer of spheres. For this reason, it appears that while both the vacuum edges of the mesa and the hard edges of the well can template single crystalline block copolymer arrays via graphoepitaxy, for technological applications, the well structures will be far more useful since one can reliably fill them with a layer of spheres.

Evolution of Islands and Holes. By using real-time SFM on a heat stage, it is possible to observe directly the evolution of the islands and holes. A PS−PVP film spun-coat from toluene, released onto the surface of a water bath, and retrieved on top of a patterned silicon grating is initially disordered. Within 10 min at a temperature of 180 °C, surface structures are evident, indicating that the spherical nanodomains have formed and a quantized film thickness is now required. Figure 5 shows a series of images depicting the early stages of coarsening of a PS−PVP film with an initial thickness of 42 nm on a grating with a periodicity of 20 μm. The 10 μm wide mesas and wells are seen as broad stripes running diagonally through the 40 μm by 40 μm square SFM images. While the film was initially smooth, holes 27 nm deep appeared within 10 min of annealing on the heat stage of the SFM, revealing the underlying PS−PVP brush. As shown in Figure 5a, holes initially appear on both the mesas and wells of the substrate surface relief structure. The fact that holes appear to achieve their full depth virtually instantly indicates that the process of order formation is very rapid. The holes make up approximately 22% of the total area of the film, as expected since the 42 nm thick film accounts for one brush layer plus 0.8α.

As discussed in the previous section, it is energetically advantageous to fill the well with material at the expense of material on the mesa so that the entire surface will appear flat. Over the next 500 min the holes in both the mesa and well coarsen mostly by coalescence (as has been observed in comparable lamellar films). Since the wells act as sinks, however, material is moved preferentially to the well edges from the mesa. The total area of the holes on the mesa increases while the well appears to narrow. After 600 min of annealing at 180 °C (not shown), enough material has been transported from the mesas to the well edges that the holes now form a bicontinuous structure on the mesa. For the next 800 min, the raised portion of the bicontinuous structure on the mesa will thin as more material is moved to the

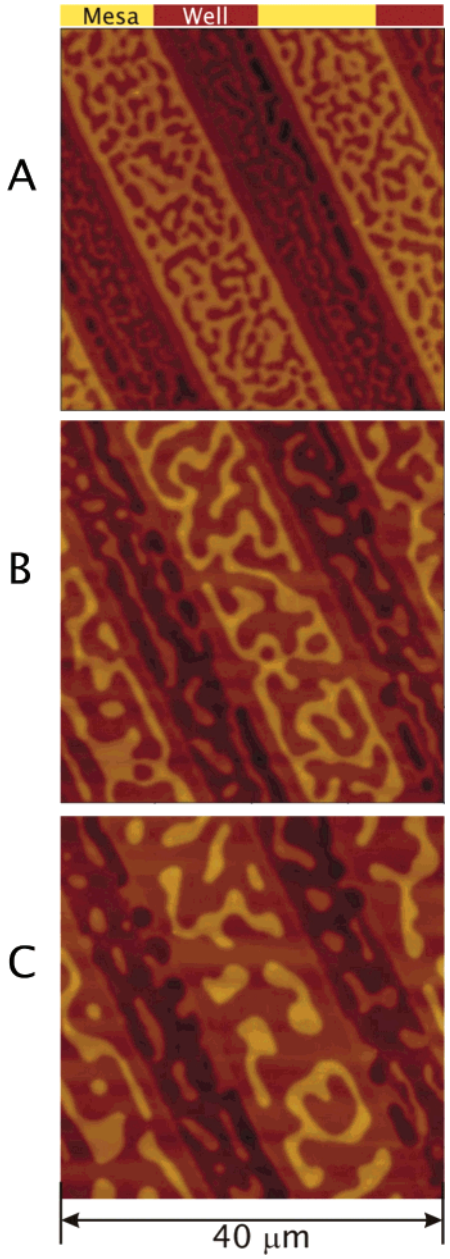

Figure 5. A time series of 40 μm square SFM images demonstrates the coarsening of island and hole structures from a film originally cast at slightly less than the natural thickness for a single layer of spheres. All images were taken at 180 °C on a heat stage microscope with height scale 75 nm. (A) After 10 min above T_g, holes revealing the brush in a single layer of spheres have appeared on both mesas (bright stripes) and wells (darker stripes). (B) At 900 min, the mesa pattern is now a bicontinuous matrix of islands and holes. (C) At 2300 min of annealing, only isolated islands exist on the mesas.

well edge, and the average width of the stripe at the well edge increases. Figure 5b demonstrates that after 900 min of annealing there is a stripe of the intermediate height at the mesa/well edge with an average width of 1.5 μm that indicates areas made up of a brush covered mesa on one side of the edge and a well filled with one layer of spheres on the well side. This stripe will increase in width as the bicontinuous structure thins.

After a total annealing time of 1300 min, the bicontinuous structure has thinned enough to break up into individual islands on the mesa. This is a typical result when the wide well is very underfilled. These islands

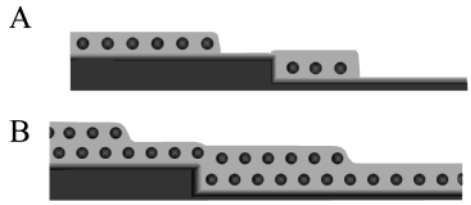

Figure 6. Schematic of two distinct regimes of island dissolution. (A) When islands are formed directly on the PS−PVP brush on the mesa, chains must diffuse across the brush to reach the sink. Once in the well, the chains may form either a new sphere at the edge or diffuse across the spherical domains to the free edge of the island in the well. (B) When the islands are formed on top of another layer of spheres, material may be incorporated into the underlying layer of spheres.

will then shrink as more material is moved to the well edge until the mesa contains only a brush and the well is as full as possible. Figure 5c demonstrates that after 2300 min of annealing this final process is still not complete. The islands shrink in radius while their centers remain stationary. There is no rigid translation of the entire island or any indication of groupings of spheres separating from the island during this shrinking process. This evidence indicates that transport of block copolymer from the mesas into the well is accomplished by the transport of individual block copolymer chains. In order for a chain to move from an island on the mesa to the well edge, it must traverse across a brush layer. Since the PS−PVP brush is relatively dense and strongly adsorbed to the underlying SiO_2 surface, it is unlikely that the chain will get trapped in the brush on the way across.

Shrinkage of Individual Islands. Island structures normally coarsen by the growth of larger domains at the expense of smaller ones. In general, descriptions of the coarsening process focus on the nature of the exchange of material between the islands and the surroundings. The movement of material from the smaller islands is driven by the edge surface tension of the 2-D islands so over time there is a decrease in the total length of island edges. The characteristic area of the islands, A, should decrease following a power law with time ($A \sim (t_f - t)^c$ where t_f is the time at which the island disappears).[38,39,49]

In the case of a topographically patterned substrate, the step edge acts as a very large island and absorbs all the surrounding islands. By observing individual islands on the mesa and in the well, the rate of shrinkage can be quantified. As shown in Figure 6, there are two distinct scenarios in which chains will move from an island toward the absorbing edge: (a) the film contains less than one complete layer of spheres (th < 47 nm), and chains must be transported across the brush that exists at the edge of the mesa; (b) there is more than one layer of spheres (th > 47 nm) so the movement of material from mesa to the edge in the well is across another complete array of spheres.

For a sample with th = 42 nm (case a above), after about 3500 min of annealing, islands exist in the center of the mesas and wells, as shown in the 40 μm by 40 μm SFM image in Figure 7a. The footprint area (A) of a number of islands (marked with black symbols) was tracked over the next 1500 min. A plot of island area vs time is useful in determining the rate at which material is transported across this brush to the sink at the edge of the well. The islands tracked in Figure 7

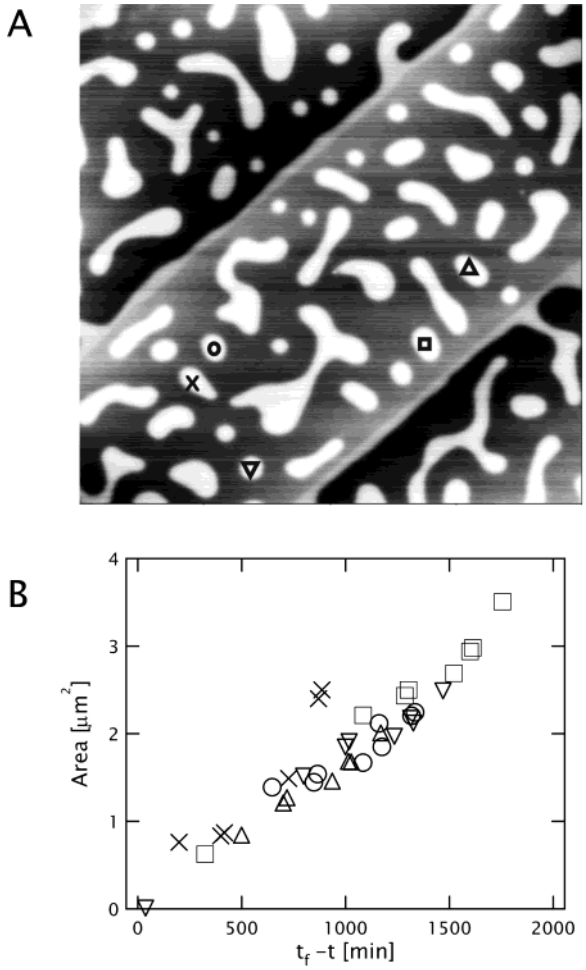

Figure 7. (A) Shrinkage of individual islands (indicated by symbols on the image) on top of a brush is observed in real time by SFM as shown in this 40 μm square image. (B) The area of individual islands decreases linearly with $t_f - t$. The various symbols correspond to the indicated islands on 15 μm wide mesas showing that the shrinkage rate on the brush does not depend on island position.

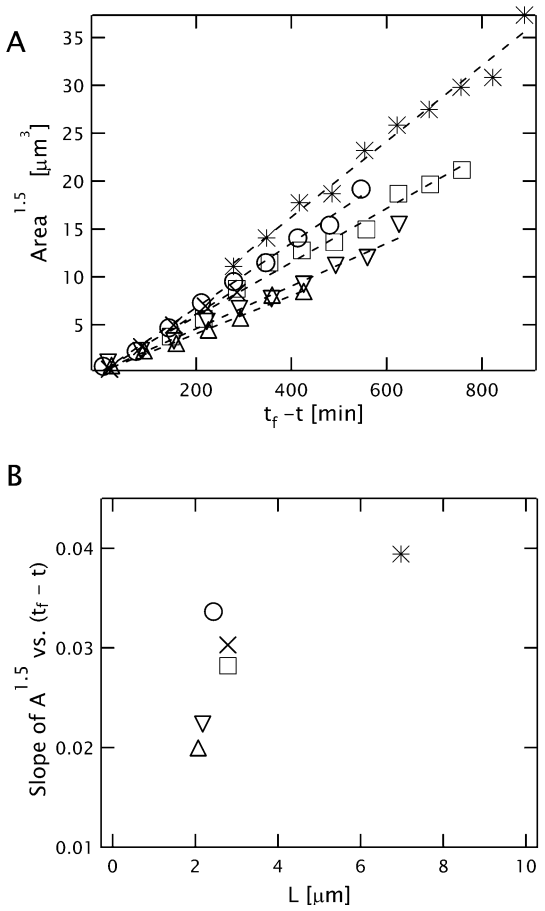

Figure 8. (A) Islands on top of a complete layer of spheres shrink such that $A \sim (t_f - t)^{2/3}$. The various symbols again indicate islands with differing distances, L, from the absorbing boundary and linear least-squares fits are drawn with dotted line. (B) The islands farther from the absorbing boundary (larger L) shrink more quickly than those closer to it.

were all of relatively small size so that they disappeared completely within the total annealing time of 5000 min of this study. The islands, however, were not uniformly sized or uniformly spaced from the edge of the layer of spheres in the well (the absorbing boundary). It is useful to extrapolate A vs time plots to find the apparent time of final disappearance, t_f. The quantity $t_f - t$ then represents the remaining "life" of the islands. It is significant that if the island area, A, is plotted vs $t_f - t$, as in Figure 7b, all of the data sets collapse into a single straight line. Thus, the shrinkage rate of the islands is constant, independent of the island radius or its distance from the absorbing boundary. This is not what one would expect for a case in which the transport of material was limited by the rate of diffusion of chains across the brush between the islands and the well edge.

The diffusion across the brush may be so rapid that the concentration profile in the brush outside the island is that in equilibrium with the straight edge of the well; i.e., the concentration gradient from the island to the well edge approaches zero. In this case, the shrinkage of an island is limited by the kinetics of detachment of chains from its edges. The flux from this island is proportional to the difference between the concentration of chains in the brush that would be in equilibrium with the island of radius, R, and that in the brush in equilibrium with the flat edge of the well. For relatively large values of R such that $\mu_{island}/k_bT = \gamma_{edge}N/R\rho k_bT < 1$ the flux is proportional to the circumference of the island times $\gamma_{edge}N/R\rho k_bT$ and thus does not depend on R. The area of the island in this situation should therefore decrease linearly with time, as observed both here and for atomic layer islands on a Si(001) surface.[49]

When the island sits on top of another layer of spheres, instead of the brush, there are many more mechanisms available both for the detachment of material from the island and the movement of this material to the well edge. Now it is possible for chains or entire spheres to leave the island through the entire area of the island footprint. We observe a film with $th = 55$ nm ($th = \beta + 1.3\alpha$) in which islands are formed by the partial second layer of spheres. After approximately 4000 min of annealing, small islands exist in the middle of the mesas and wells. The area of several of these islands of varying size and location were monitored for an additional 500 min via optical microscopy. In this case, we observe that $c = {}^2/_3$ and a plot of $A^{3/2}$ vs $t_f - t$ is linear, as shown in Figure 8. This is expected if diffusion limits the speed of the shrinkage process (Lifshitz−Slyozov shrinkage).[50] In this case, the equilibration of the chemical potential of block copolymer at the edges of the island is much faster than that of the concentration profile between the island and the mesa edge. Since the chemical potential is continuous across

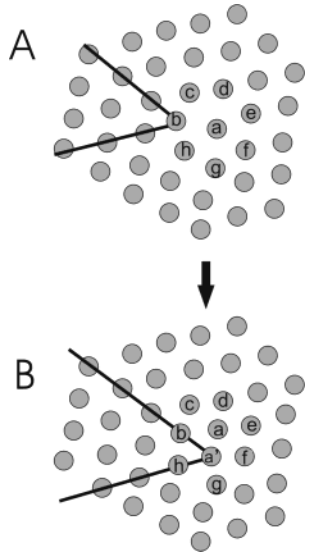

Figure 9. (A) A schematic drawing of a dislocation indicates that the 7-fold coordinate sphere ($7 - a$) is more widely separated from its nearest neighbors and the two extra half rows of material (black lines) intersect at a 5-fold coordinate sphere ($5 - b$). (B) If the location of the original sphere a is now occupied by two spheres (a and a'), the dislocation climbs one lattice spacing. Sphere f is now a 7 and sphere a' is a 5.

the island edges, this diffusion-limited shrinkage should have $c = {}^2/_3$.

The diffusion of chains in the spherical morphology requires "activated hopping" of chains from one sphere to another. In each hop, there are new contacts made between the monomers (in this case styrene and vinylpyridine) so the diffusion coefficient $\langle D \rangle \sim \exp(-\chi N_{PVP})$, where χ is the Flory−Huggins interaction parameter and N_{PVP} is the length of the smaller of the two blocks. The block copolymer used in this study is experimentally observed to have $\langle D \rangle \approx 4 \times 10^{-14}$ cm^2/s at 180 °C,[51] so a chain that is 1 μm away from the edge will take about 4000 min to arrive. Experimentally, however, the dissolution of an island that is in the second layer of spheres is much faster even than that in a layer of spheres on a brush. A 4 μm^2 island located 3.8 μm from the absorbing edge will dissolve in only 400 min. One would also expect that if a chain is to diffuse from the island all the way to the sink, the islands nearer to the sink should dissolve faster than those farther away. As shown in Figure 8b, this expected dependence on distance from the edge (L) is not observed; in fact, it appears that islands farther from the edge disappear more quickly. It is unlikely, therefore, that the diffusive transport through the bottom layer of spheres is alone responsible for the transport of material from the island to the well.

If the island dissolution is not occurring via the movement of individual chains all the way to the sink, there must be some concerted motion of the spheres themselves. There is, however, no evidence for the diffusion of entire spherical nanodomains in three-dimensional samples of this block copolymer.[52] It is still possible, however, for there to be some slippage of rows of spheres in a two-dimensional lattice. At the core of a dislocation in two dimensions (where the two extra half rows of material emphasized by bold lines intersect as schematically diagrammed in Figure 9a), there is one 5-fold sphere (b) and one 7-fold coordinated sphere (a). It is obvious from this diagram that there is a good deal of extra space around the 7-fold site. The imposition of an extra sphere here would extend each of the half rows by one lattice spacing. This motion is what is called dislocation climb in atomic materials and has been demonstrated in magnetic bubble arrays.[53] The surrounding material would be pushed to either side to accommodate the extra sphere, resulting in the movement of all the surrounding spheres by less than half a lattice spacing. This is important, however, since at the edge of the mesa this motion will drive more spheres off of the mesa and onto the well.

During the annealing process, the arrangement of the spherical nanodomains in the underlying layer also evolves through the annihilation of dislocations and the sweeping of a dominant grain boundary away from the mesa edge. The single layer of spheres is a 2-D system in which, after 72 h of annealing at 180 °C, the dislocation density is approximately $1/\mu$m^2 within the 2 μm wide stripe near the well edge (so the standard 4 μm^2 island would have at least four dislocation sites).[43] More than 2 μm from the wall, the array of spheres is polycrystalline, and grain boundaries occur approximately every 0.5 μm. The grain boundaries are made up of strings of 5- and 7-fold coordinated spheres (disclinations). Since the number of defects is greater near the center of the mesa than near the edges,[47] it is not surprising that the islands in the center of the mesa shrink more quickly than those near the edges. If this is the case, the rate of shrinkage of individual islands is dependent on the number of dislocations ($\rho_d A$) in the underlying layer of spheres times the chemical potential driving force given in eq 2 ($\mu_{island} = \gamma_{edge} N/(R\rho)$) so that

$$\frac{dA}{dt} = -k\rho_d R = -k\rho_d\left(\frac{A}{\pi}\right)^{1/2} \tag{4}$$

where ρ_d is the density of dislocations (including those seen in grain boundaries). We assume that k is a rate constant for the insertion of a sphere and also includes the constants from eq 2. The density of dislocations, however, decreases with time as dislocations of opposite sign annihilate and the grain size increases. We will assume that it decreases as a power law in time, $\rho_d \sim \rho_0 t^{-\nu}$.[43,54] As a result

$$A^{1/2} = \frac{k\rho_0}{\sqrt{4\pi}}(t_f - t)^{1-\nu} \tag{5}$$

and from Figure 8, we know that

$$A^{3/2} \sim t_f - t \tag{6}$$

By substituting eq 6 into eq 5, we find that for this mechanism to give agreement with our experimental data $\nu = {}^2/_3$ and thus $\rho_d \sim t^{-2/3}$.

If this dislocation climb mechanism is responsible for the island shrinkage, we assume that the motion of the surrounding spheres is much faster than the formation or movement of a single sphere into the bottom layer. This layer-to-layer motion, however, could occur by a variety of mechanisms: an entire sphere could move from the island to the dislocation core underneath, or chains from the island could move to nucleate a new sphere at the dislocation core. If the mechanism of sphere motion from the island layer into the bottom layer of spheres is by the hopping diffusion of individual chains, then the process should be limited by the time

of this hop. Yokoyama et al. have demonstrated that the characteristic time scale for a chain to "hop" from one layer of spheres to another is roughly 800 min for a 117 000 g/mol PS−PVP diblock copolymer with $f_{PVP} \sim 0.12$ (significantly larger than our diblock).[55] If we scale this characteristic time by $\exp(-\chi N_{PVP})$, we find that this characteristic time is roughly 12 min for our block copolymer. This is not a reasonable number since the time to total disappearance, t_f, for a typical island is approximately 400 min. If the hexagonal array of spheres in the island is in registry with the underlayer, there will be one sphere directly above the 7-fold site in the underlying dislocation. This sphere would have to move less than one lattice spacing to slip down into the site below. Since the spheres within the island are under considerable pressure, we assume that this motion would be quite fast and could account for the movement of material from the island into the dislocation core.

Conclusions

We observe the coarsening of surface structures similar to that of the islands and holes observed for lamellar block copolymers. By using surface topographies that act as sinks, the movement of material from one region of the film to another can be directly observed. Material can be moved from a raised mesa to a well edge without the introduction of any new line length. As a result, if the initial spun-cast film thickness is even slightly under the natural thickness, material will shrink away from the edges of the mesas to preferentially fill the well. Similarly, if the initial thickness is slightly more than the natural thickness, a second layer of spheres will be added to the well edge. As a result, if a film is cast such that only 80% of the surface can be covered with spheres after the brush has formed, holes in a single layer of spheres appear to reveal the underlying brush. These holes on the mesa surface coalesce and grow as material is transferred to the well edge and eventually form a bicontinuous structure. The bicontinuous structure on the mesa then narrows as material is moved to the well edge until finally it breaks into individual islands. These islands then shrink as chains detach from the island and diffuse across the surrounding brush on the mesa to the edge of the layer of spheres in the well. This process is limited by the attachment/detachment process of the chains from the island, and the area of individual islands, A, decreases linearly with time.

If the islands are formed on top of another layer of spheres, however, the island shrinkage occurs much more quickly. This speed is surprising since the diffusion coefficient of a chain across the brush should be faster than that across a layer of nanodomains. We speculate that this speed is due to the ability of dislocations in the underlayer of spheres to absorb additional material from above, inserting extra spheres at the end of their extra half rows (climb) and thus shifting more spheres into this layer from the mesa to the well.

Acknowledgment. We gratefully acknowledge the financial support of the U.S. National Science Foundation DMR Polymers Program under Grant DMR 98-03738, the NSF National Nanofabrication Users Network REU Program for support of K.E.S., and the Corning Foundation for fellowship support of R.A.S. This work also made use of MRL Central Facilities supported by the NSF MRSEC Program under Award DMR00-80034. The assistance of Tom Mates for SIMS is also greatly appreciated.

References and Notes

(1) Mansky, P.; Harrison, C. K.; Chaikin, P. M.; Register, R. A.; Yao, N. *Appl. Phys. Lett.* **1996**, *68*, 2586−2588.
(2) Park, M.; Harrison, C.; Chaikin, P. M.; Register, R. A.; Adamson, D. H. *Science* **1997**, *276*, 1401−1404.
(3) Li, R. R.; Dapkus, P. D.; Thompson, M. E.; Jeong, W. G.; Harrison, C.; Chaikin, P. M.; Register, R. A.; Adamson, D. H. *Appl. Phys. Lett.* **2000**, *76*, 1689−1691.
(4) Guarini, K. W.; Black, C. T.; Milkove, K. R.; Sandstrom, R. L. *J. Vac. Sci. Technol., B* **2001**, *19*, 2784−2788.
(5) Black, C. T.; Guarini, K. W.; Milkove, K. R.; Baker, S. M.; Russell, T. P.; Tuominen, M. T. *Appl. Phys. Lett.* **2001**, *79*, 409−411.
(6) Cheng, J. Y.; Ross, C. A.; Chan, V. Z. H.; Thomas, E. L.; Lammertink, R. G. H.; Vancso, G. J. *Adv. Mater.* **2001**, *13*, 1174−1178, 1125.
(7) Kim, H. C.; Jia, X. Q.; Stafford, C. M.; Kim, D. H.; McCarthy, T. J.; Tuominen, M.; Hawker, C. J.; Russell, T. P. *Adv. Mater.* **2001**, *13*, 795−797.
(8) Sohn, B. H.; Seo, B. H. *Chem. Mater.* **2001**, *13*, 1752−1757.
(9) Watkins, J. J.; McCarthy, T. J. *Chem. Mater.* **1995**, *7*, 1991+.
(10) Thurn-Albrecht, T.; Schotter, J.; Kastle, C. A.; Emley, N.; Shibauchi, T.; Krusin-Elbaum, L.; Guarini, K.; Black, C. T.; Tuominen, M. T.; Russell, T. P. *Science* **2000**, *290*, 2126−2129.
(11) Bates, F. S.; Fredrickson, G. H. *Phys. Today* **1999**, *52*, 32−38.
(12) Morkved, T. L.; Lu, M.; Urbas, A. M.; Ehrichs, E. E.; Jaeger, H. M.; Mansky, P.; Russell, T. P. *Science* **1996**, *273*, 931−933.
(13) Mansky, P.; Russell, T. P.; Hawker, C. J.; Pitsikalis, M.; Mays, J. *Macromolecules* **1997**, *30*, 6810−6813.
(14) Mansky, P.; DeRouchey, J.; Russell, T. P.; Mays, J.; Pitsikalis, M.; Morkved, T.; Jaeger, H. *Macromolecules* **1998**, *31*, 4399−4401.
(15) Hahm, J.; Sibener, S. J. *Langmuir* **2000**, *16*, 4766−4769.
(16) Yang, X. M.; Peters, R. D.; Nealey, P. F.; Solak, H. H.; Cerrina, F. *Macromolecules* **2000**, *33*, 9575−9582.
(17) Park, C.; De Rosa, C.; Thomas, E. L. *Macromolecules* **2001**, *34*, 2602−2606.
(18) Yang, X. M.; Peters, R. D.; Nealey, P. F.; Solak, H. H.; Cerrina, F. *Macromolecules* **2000**, *33*, 9575−9582.
(19) Segalman, R. A.; Yokoyama, H.; Kramer, E. J. *Adv. Mater.* **2001**, *13*, 1152−1155.
(20) Fasolka, M. J.; Mayes, A. M. *Annu. Rev. Mater. Res.* **2001**, *31*, 323−355.
(21) Fredrickson, G. H.; Helfand, E. *J. Chem. Phys.* **1987**, *87*, 697−705.
(22) Coulon, G.; Russell, T. P.; Deline, V. R.; Green, P. F. *Macromolecules* **1989**, *22*, 2581−2589.
(23) Russell, T. P.; Coulon, G.; Deline, V. R.; Miller, D. C. *Macromolecules* **1989**, *22*, 4600−4606.
(24) Anastasiadis, S. H.; Russell, T. P.; Satija, S. K.; Majkrzak, C. F. *Phys. Rev. Lett.* **1989**, *62*, 1852−1855.
(25) Menelle, A.; Russell, T. P.; Anastasiadis, S. H.; Satija, S. K.; Majkrzak, C. F. *Phys. Rev. Lett.* **1992**, *68*, 67−70.
(26) Foster, M. D.; Sikka, M.; Singh, N.; Bates, F. S.; Satija, S. K.; Majkrzak, C. F. *J. Chem. Phys.* **1992**, *96*, 8605−8615.
(27) Fasolka, M. J.; Harris, D. J.; Mayes, A. M.; Yoon, M.; Mochrie, S. G. J. *Phys. Rev. Lett.* **1997**, *79*, 3018−3021.
(28) Rockford, L.; Liu, Y.; Mansky, P.; Russell, T. P.; Yoon, M.; Mochrie, S. G. J. *Phys. Rev. Lett.* **1999**, *82*, 2602−2605.
(29) Heier, J.; Sivaniah, E.; Kramer, E. J. *Macromolecules* **1999**, *32*, 9007−9012.
(30) Joly, S.; Raquois, A.; Paris, F.; Hamdoun, B.; Auvray, L.; Ausserre, D.; Gallot, Y. *Phys. Rev. Lett.* **1996**, *77*, 4394−4397.
(31) Heier, J.; Genzer, J.; Kramer, E. J.; Bates, F. S.; Walheim, S.; Krausch, G. *J. Chem. Phys.* **1999**, *111*, 11101−11110.
(32) Coulon, G.; Ausserre, D.; Russell, T. P. *Abstr. Pap. Am. Chem. Soc.* **1989**, *197*, 198-Poly.
(33) Coulon, G.; Collin, B.; Ausserre, D.; Chatenay, D.; Russell, T. P. *J. Phys. (Paris)* **1990**, *51*, 2801−2811.
(34) Coulon, G.; Ausserre, D.; Russell, T. P. *J. Phys. (Paris)* **1990**, *51*, 777−786.
(35) Coulon, G.; Collin, B.; Chatenay, D.; Gallot, Y. *J. Phys. Ii* **1993**, *3*, 697−717.

(36) Collin, B.; Chatenay, D.; Coulon, G.; Ausserre, D.; Gallot, Y. *Macromolecules* **1992**, *25*, 1621−1622.
(37) Maaloum, M.; Ausserre, D.; Chatenay, D.; Coulon, G.; Gallot, Y. *Phys. Rev. Lett.* **1992**, *68*, 1575−1578.
(38) Bassereau, P.; Brodbreck, D.; Russell, T. P.; Brown, H. R.; Shull, K. R. *Phys. Rev. Lett.* **1993**, *71*, 1716−1719.
(39) Bassereau, P.; Brodbeck, D.; Russell, T. P.; Brown, H. R.; Shull, K. R. *Phys. Rev. Lett.* **1995**, *74*, 4961−4961.
(40) Grim, P. C. M.; Nyrkova, I. A.; Semenov, A. N.; Tenbrinke, G.; Hadziioannou, G. *Macromolecules* **1995**, *28*, 7501−7513.
(41) Heier, J.; Kramer, E. J.; Groenewold, J.; Fredrickson, G. H. *Macromolecules* **2000**, *33*, 6060−6067.
(42) Yokoyama, H.; Mates, T. E.; Kramer, E. J. *Macromolecules* **2000**, *33*, 1888−1898.
(43) Segalman, R. A.; Hexemer, A.; Hayward, R. C.; Kramer, E. J. *Macromolecules* **2003**, *36*, 3272−3288.
(44) Rayleigh, L. *Proc. London Math. Soc.* **1878**, 4.
(45) Brochard-Wyart, F.; Redon, C. *Langmuir* **1992**, *8*, 4−2329.
(46) Reiter, G.; Sharma, A. *Phys. Rev. Lett.* **2001**, *87*, 166103.
(47) Segalman, R. A.; Hexemer, A.; Kramer, E. J. *Macromolecules*, in press.
(48) Segalman, R. A.; Hexemer, A.; Kramer, E. J., submitted for publication.
(49) Theis, W.; Bartelt, N. C.; Tromp, R. M. *Phys. Rev. Lett.* **1995**, *75*, 3328−3331.
(50) Lifshitz, I. M.; Slyozov, V. V. *J. Phys. Chem. Solids* **1961**, *19*, 33−50.
(51) Yokoyama, H.; Kramer, E. J. *Macromolecules* **1998**, *31*, 7871−7876.
(52) Yokoyama, H.; Kramer, E. J.; Hajduk, D. A.; Bates, F. S. *Macromolecules* **1999**, *32*, 3353−3359.
(53) Seul, M.; Murray, C. A. *Science* **1993**, *262*, 558−560.
(54) Trawick, M.; Angelscu, D.; Chaikin, P. M.; Sebastian, J.; Register, R.; Adamson, D.; Harrison, C. In *Bulletin of the American Physical Society March Meeting*; Indianapolis, IN, 2002; Vol. 47, Part II, p 970.
(55) Yokoyama, H.; Kramer, E. J.; Rafailovich, M. H.; Sokolov, J.; Schwarz, S. A. *Macromolecules* **1998**, *31*, 8826−8830.

MA025879C